

Electronic Supplementary Information

Pyridine functionalized silver nanosheets for nitrate electroreduction

Han-Yue Yang,^a Kai-Yue He,^a Xuan Ai,^{*a} Xue Liu,^b Yun Yang,^{*b} Shi-Bin Yin,^c Pu-Jun Jin^a and Yu Chen^a

^a *School of Materials Science and Engineering, Shaanxi Normal University, Xi'an 710062, Shaanxi, P. R. China.*

^b *Nanomaterials and Chemistry Key Laboratory, Wenzhou University, Wenzhou 325035, P. R. China.*

^c *Guangxi Key Laboratory of Electrochemical Energy Materials, School of Chemistry and Chemical Engineering, Guangxi University, Nanning 530004, P. R. China.*

**Corresponding authors*

E-mail addresses: yunyang@wzu.edu.cn (Y. Yang), aixuanchem@outlook.com (X. Ai)

1. Experimental Section

1.1 Physical characterization

The morphology, crystal structure, chemical composition, thickness, chemical state and surface-bonded organic molecules of the electrocatalysts were characterized by scanning electron microscopy (SEM, SU-8020), field emission ultra-high resolution transmission electron microscopy (TEM, JEM-2800), X-ray diffractometry (XRD, DX-2700), energy dispersive X-ray energy spectrometry (EDX), atomic force microscopy (AFM, Dimension ICON), X-ray photoelectron spectroscopy (XPS, AXIS ULTRA), infrared spectroscopy (IR, VERTEX 70v) and thermogravimetric analysis (TGA, STA 449 F5). NH_3 concentration and NO_2^- concentration measurements were completed using previously reported methods on an ultraviolet-visible spectrophotometer (UV-vis, UV-2600).¹⁻³

1.2. Electrochemical measurements

Linear scanning voltammetry (LSV) and chronoamperometry (AC) were performed on a CHI-660E electrochemical workstation at $30 \pm 1^\circ\text{C}$. In the three-electrode system, a glassy carbon electrode drop-coated with electrocatalyst was used as the working electrode, a saturated glycolic electrode as the reference electrode, and a carbon rod as the counter electrode. The electrode potential was converted to the corresponding reversible hydrogen electrode potential (RHE) according to the equation $E_{\text{RHE}} = E_{\text{SCE}} + 0.059 \text{ pH} + 0.242 \text{ V}$.

The 2 mg of electrocatalyst was dispersed in a 1 mL mixture of deionized water and isopropanol (deionized water:isopropanol = 8:2), sonicated for 10 min to ensure uniform dispersion. And 4 μL of electrocatalyst ink was dropped onto the surface of a clean glassy carbon electrode (3 mm in diameter). After dried for 15 min, 4 μL of Nafion solution (5 wt%) was dropped onto the surface of the electrode loaded with electrocatalyst to immobilize the catalyst, and then dried again. All electrolytes were freshly prepared, and the water source for the solutions was ultrapure water (conductivity of $18.25 \text{ M}\Omega \cdot \text{cm}^{-1}$). Electrochemical tests were respectively performed in argon (Ar)-saturated 1 M KOH solution and Ar-saturated 1 M KOH solution containing 0.05 M KNO_3 .

1.3 The Faradaic efficiency of NO₃RR and NH₃ yield rate

The chronoamperometry tests of NO₃RR were performed using an H-type electrolyzer (Fig. S3) with Ar-purged 1 M KOH + 0.05 M KNO₃ solution and 1 M KOH solution (40 mL in each compartment). Nafion 117 membrane was used to separate two compartments of H-type electrolyzer, which was permeable to protons. The Faradaic efficiency for NH₄⁺ production was defined as charge converted to NH₄⁺ divided by the total charge passed through the electrodes during the electrolysis (Q), which was calculated according to the following equation 1:

$$\text{Faradaic efficiency} = \frac{8F \times c_{\text{NH}_3} \times V}{M_{\text{NH}_3} \times Q} \times 100\% \quad \text{equation 1}$$

where c_{NH_3} is the mass concentration of NH₃ (aq); V is the volume of electrolyte in the cathode chamber (40 mL); M_{NH_3} is the molar mass of NH₃; F is Faraday's constant (96485 C mol⁻¹); Q is the total charge through the electrode.

The NH₄⁺ yield was calculated by following equation 2:

$$\text{Yield rate} = \frac{c_{\text{NH}_3} \times V}{m \times t} \quad \text{equation 2}$$

where c_{NH_3} is the mass concentration of NH₃(aq); V is the volume of electrolyte in the cathode chamber (40 mL); m and t are the electrocatalyst mass and the time to test the timing current, respectively.

1.3 Determination of NH₄⁺-N and nitrite-N

Phenol-hypochlorite method was used to detect the NH₃ concentration. The solution preparation method is as follows: (1) Phenol alcohol reagent: 10 g of phenol dissolved in 100 mL of 95% ethanol; (2) Na₂[Fe(CN)₅NO] solution: dissolve 1.25 g of Na₂[Fe(CN)₅NO] in ultrapure water (conductivity of 18.25 MΩ · cm⁻¹) and dilute to 250 mL in a brown volumetric flask; (3) Alkaline complexing agent: dissolve 50 g of trisodium citrate and 2.5 g of sodium hydroxide in ultrapure water, and dilute to 250 mL in a volumetric flask; (4) Oxidant solution: add 20 mL of alkaline complexing agent to 5 mL of sodium hypochlorite, which needs to be freshly configured daily.

The corresponding standard curve was obtained by UV-vis curves for known concentration of NH_4^+ in 0.1 M KOH: (1) a series of standard solutions were prepared by dissolving different amount of $(\text{NH}_4)_2\text{SO}_4$ in 0.1 M KOH solution; (2) add 0.4 mL of phenol alcohol reagent, 0.4 mL of $\text{Na}_2[\text{Fe}(\text{CN})_5\text{NO}]$ solution and 1 mL oxidant solution to 10 mL of different concentration $(\text{NH}_4)_2\text{SO}_4$ standard solutions, and then place the mixed solutions in the dark for at least 1 h. (3) measure the absorbance of mixed solution at 650 nm with UV-vis spectrophotometer, and the obtained values are corrected with the blank value.

After running chronoamperometry test for 3 h, 1 mL of electrolyte were taken from electrolyzer, put it into the centrifuge tube and diluted to 10 mL with water. Then 0.4 mL of phenol alcohol reagent, 0.4 mL of $\text{Na}_2[\text{Fe}(\text{CN})_5\text{NO}]$ solution and 1 mL oxidant solution were added in solution and place the mixed solutions in the dark for at least 1 h. Finally, $\text{NH}_4^+\text{-N}$ concentration was calculated according to the UV-vis curve and standard curve.

Griess test was used to analyze the nitrite concentration. The solution preparation method is as follows: (1) Sulfonamide solution: dissolve 1.0 g sulfonamide, and 10 mL hydrochloric acid in 70 mL ultrapure water and a dilute to 100 mL in a volumetric flask; (2) N-(1-naphthyl) ethylenediamine dihydrochloride solution: dissolve 0.1 g N-(1-naphthyl) ethylenediamine dihydrochloride in ultrapure water and a dilute to 100 mL in a brown volumetric flask.

The corresponding standard curve was obtained by UV-vis curves for known concentration of NO_2^- in 0.1 M KOH: (1) a series of standard solutions were prepared by dissolving different amount of NaNO_2 in 0.1 M KOH solution; (2) add 1 mL of sulfonamide solution to 10 mL of different concentration NaNO_2 standard solutions, and then place the mixed solutions at least 8 min; (3) add 1 mL of s N-(1-naphthyl) ethylenediamine dihydrochloride solution to above solution, and then place the mixed solutions at least 10 min; (3) measure the absorbance of mixed solution at 540 nm with UV-vis spectrophotometer, and the obtained values are corrected with the blank value.

After running chronoamperometry test for 3 h, 1 mL of electrolyte were taken from electrolyzer, put it into the centrifuge tube and diluted to 10 mL with water. Then 1 mL

of sulfonamide solution was added in solution and place the mixed solutions in the dark for at least 8 min. And add 1 mL of N-(1-naphthyl) ethylenediamine dihydrochloride solution to above solution, and then place the mixed solutions at least 10 min. Finally, NO_2^- concentration was calculated according to the UV-vis curve and standard curve.

2. Theoretical Section

In the present study, density functional theory (DFT) calculations were performed using the *Vienna ab initio simulation package* (VASP).^{4, 5} The Perdew-Burke-Ernzerhof (PBE) exchange correlation functional within the generalized gradient approximation (GGA) was employed, with a 400 eV cutoff for the plane-wave basis set.^{6, 7} We constructed 2×2 supercell for Ag slab model by cleaving the bulk structure along the (111) direction. The Brillouin zones were sampled using a Monkhorst-Pack grid with dimensions of $9 \times 9 \times 9$ and $3 \times 3 \times 1$ for bulk Ag and Ag(111) slab models, respectively.⁸ The convergence criteria were set at 10^{-4} eV for energy and 0.02 eV \AA^{-1} for force. To prevent interlayer interactions, a vacuum layer of 15 \AA was chosen. During the computational process, full relaxation was performed on all upper half atom layers, while the remaining layers were kept frozen.

The calculation of the NO_3RR process is based on the computational hydrogen electrode (CHE) model proposed by Nørskov.^{9, 10} The Gibbs free energy change (ΔG) for each elementary step is determined by the equation 3:

$$\Delta G = \Delta E + \Delta \text{ZPE} - T\Delta S \quad \text{equation 3}$$

where ΔE represents the total energy obtained from DFT calculations, ΔZPE and ΔS is the zero-point energy and entropy change of intermediate adsorption, respectively. T is the temperature which was set to 298 K. To avoid directly calculating the energy of charged NO_3^- , gaseous HNO_3 is selected as a reference.^{11, 12} $\Delta G(*\text{NO}_3)$ is determined by the equation 4:

$$\Delta G(*\text{NO}_3) = G(*\text{NO}_3) - G^* - G(*\text{NO}_3) + 1/2 G(\text{H}_2) + 0.392 \text{ eV} \quad \text{equation 4}$$

where $G(*\text{NO}_3)$, G^* , $G(*\text{NO}_3)$ and $G(\text{H}_2)$ are the Gibbs free energy of NO_3^- adsorbed on the substrates, substrates, gas HNO_3 , and gas H_2 , respectively. As for gas molecules, their entropy values were taken from the standard values at 298.15 K and 1 atm: $\text{TS}(\text{H}_2) = 0.41 \text{ eV}$, $\text{TS}(\text{NH}_3) = 0.60 \text{ eV}$, $\text{TS}(\text{HNO}_3) = 0.83 \text{ eV}$ and $\text{TS}(\text{H}_2\text{O}) = 0.67 \text{ eV}$.¹³

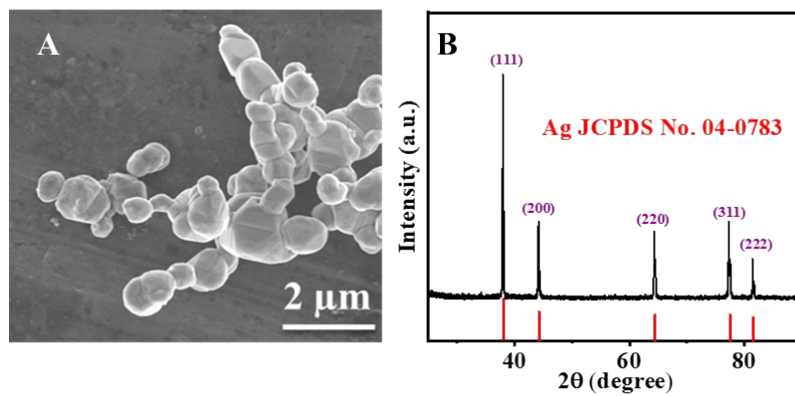


Fig. S1 (A) SEM image and (B) XRD pattern of Ag-NCs for IR test.

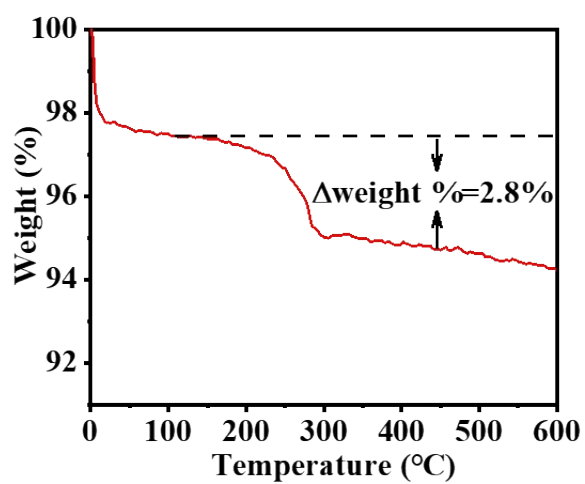


Fig. S2 Thermogravimetric analysis curve of Py-Ag NSs.

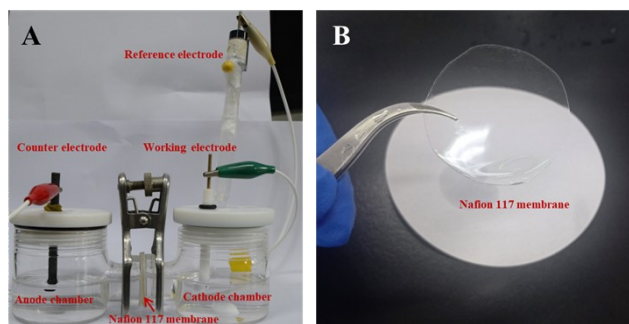


Fig. S3 Photograph illustrations of (A) H-type electrolyzer and (B) Nafion 117 membrane.

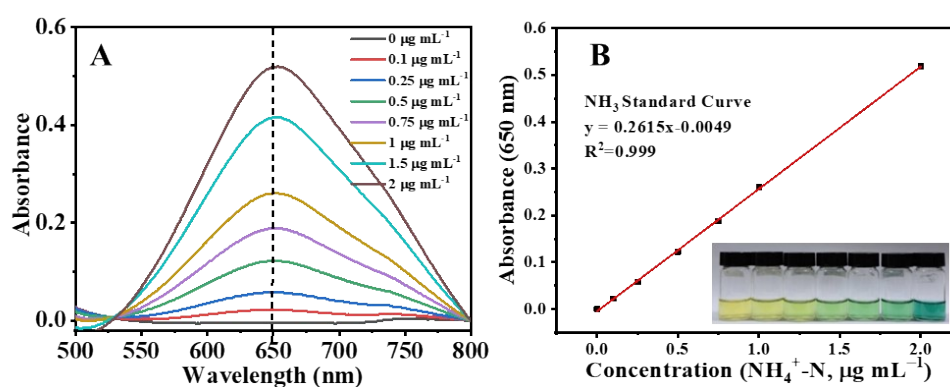


Fig. S4 (A) The UV-Vis curves of different concentration of ammonium solution at room temperature. (B) Standard curve for estimating NH_3 through NH_4^+ concentration. The fitted curve shows a good linear relationship between absorbance at 650 nm and NH_4^+ concentration ($y=0.2615x - 0.0049$, $R^2=0.999$).

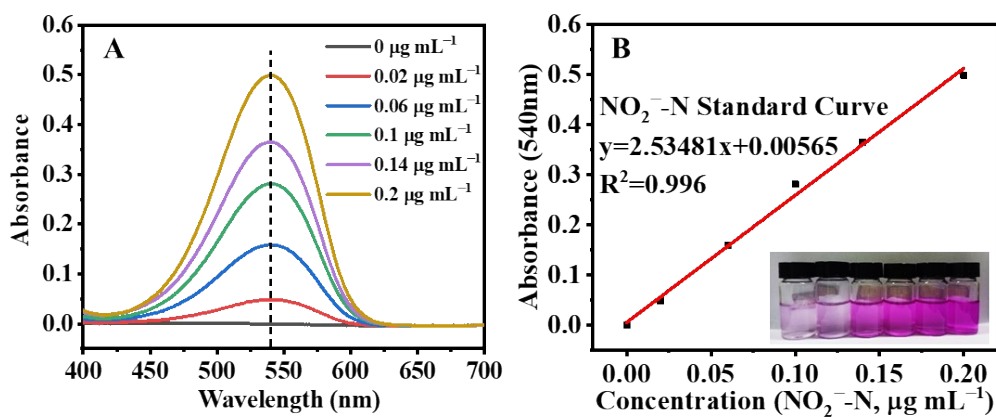


Fig. S5 (A) The UV-Vis curves of different concentration of NaNO₂ solutions at room temperature. (B) Standard curve for estimating NO₂⁻ concentration. The fitted curve shows a good linear relationship between absorbance at 540 nm and NO₂⁻ concentration ($y = 2.53481x + 0.00565$, $R^2 = 0.996$).

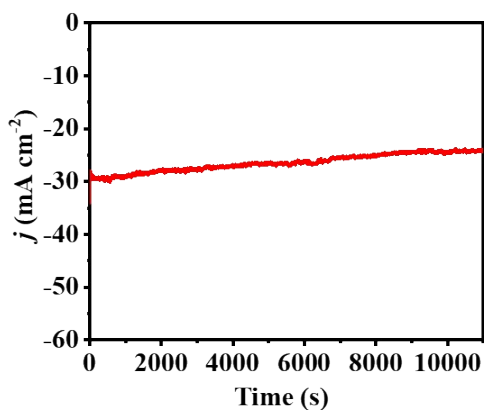


Fig. S6 Chronoamperometric curve of Py-Ag NSs on carbon cloth in 1 M KOH + 0.05 M KNO₃ solution at -0.53 V.

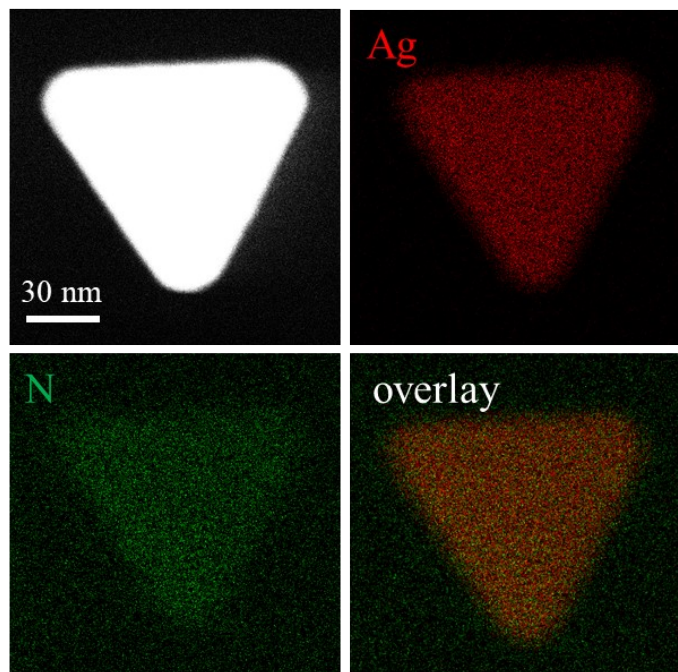


Fig. S7 HAADF-STEM-EDS maps of Py-Ag NSs after 3h chronoamperometry test for NO_3RR .

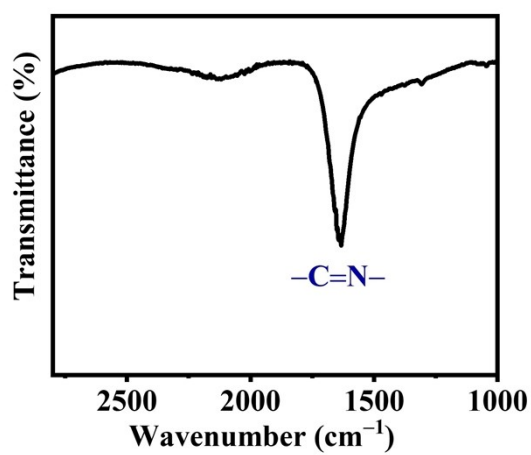


Fig. S8 IR spectra of Py-Ag NSs after 3h chronoamperometry test for NO_3RR .

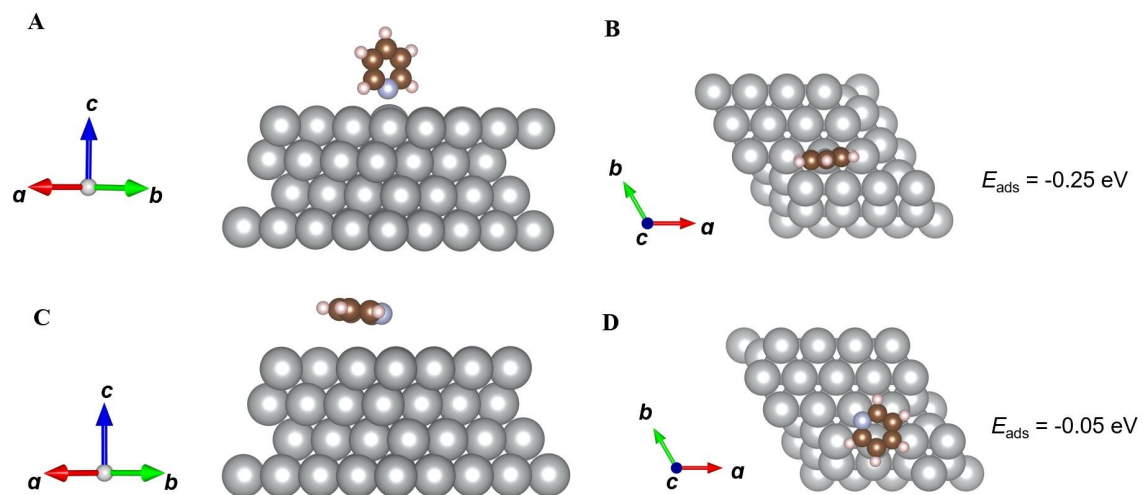


Fig. S9 (A) Side and (B) top views of Py adsorbed on Ag(111) with vertical configuration. (C) Side and (D) top views of Py adsorbed on Ag(111) with parallel configuration.

References

1. O. Brylev, M. Sarrazin, L. Roué and D. Bélanger, *Electrochim. Acta*, 2007, **52**, 6237-6247.
2. H.-M. Liu, S.-H. Han, Y. Zhao, Y.-Y. Zhu, X.-L. Tian, J.-H. Zeng, J.-X. Jiang, B. Y. Xia and Y. Chen, *J. Mater. Chem. A*, 2018, **6**, 3211-3217.
3. X.-H. Wang, Z.-M. Wang, Q.-L. Hong, Z.-N. Zhang, F. Shi, D.-S. Li, S.-N. Li and Y. Chen, *Inorg. Chem.*, 2022, **61**, 15678-15685.
4. G. Kresse and J. Furthmüller, *Comput. Mater. Sci*, 1996, **6**, 15-50.
5. G. Kresse and J. Furthmüller, *Phys. Rev. B*, 1996, **54**, 11169-11186.
6. J. P. Perdew, K. Burke and M. Ernzerhof, *Phys. Rev. Lett.*, 1996, **77**, 3865-3868.
7. P. E. Blöchl, *Phys. Rev. B*, 1994, **50**, 17953-17979.
8. H. J. Monkhorst and J. D. Pack, *Phys. Rev. B*, 1976, **13**, 5188-5192.
9. J.-X. Liu, D. Richards, N. Singh and B. R. Goldsmith, *ACS Catal.*, 2019, **9**, 7052-7064.
10. J. K. Nørskov, J. Rossmeisl, A. Logadottir, L. Lindqvist, J. R. Kitchin, T. Bligaard and H. Jónsson, *The Journal of Physical Chemistry B*, 2004, **108**, 17886-17892.
11. F. Calle-Vallejo, M. Huang, J. B. Henry, M. T. M. Koper and A. S. Bandarenka, *Phys. Chem. Chem. Phys.*, 2013, **15**, 3196-3202.
12. S. Guo, K. Heck, S. Kasiraju, H. Qian, Z. Zhao, L. C. Grabow, J. T. Miller and M. S. Wong, *ACS Catal.*, 2018, **8**, 503-515.
13. W. M. Haynes, *CRC handbook of chemistry and physics*, CRC press, 2016.